

Coupled Rotational and Translational Modes in the Mixed Molecular Crystal $\text{KBr}_{1-x}(\text{CN})_x$

A. Loidl*, R. Feile* and K. Knorr*

Institut für Physik, Universität Mainz, Mainz, W.-Germany

B. Renker

Institut für Angewandte Kernphysik, Kernforschungszentrum Karlsruhe,
Karlsruhe, W.-Germany

J. Daubert

Physik Department, TH München, Garching, W.-Germany

D. Durand

Faculté des Sciences, Université de Metz, Metz, France

J.B. Suck

Institut Max von Laue-Paul Langevin, Grenoble, France

The E_g and T_{2g} acoustic phonon modes of the molecular crystals $\text{KBr}_{0.96}(\text{CN})_{0.04}$ and $\text{KBr}_{0.86}(\text{CN})_{0.14}$ have been investigated by inelastic neutron scattering at 6, 90 and 300 K. Clear resonances due to mode-mode coupling to molecular excitations were observed. In complementary ultrasonic experiments the elastic constants were found to pass through minima as a function of temperature. The results were quantitatively explained by a model which assumes simple forms of the molecular excitation spectrum. An alternative interpretation, though being only qualitative, postulates a freezing of the CN molecules into a glass-like phase.

1. Introduction

It is well known that the resonant scattering of excitations leads to coupled modes which can be described as a mixture of the wave functions of the excitations and the scattering system. Focusing on substitutional impurities in crystals, the phonons interact with a great variety of resonant scatterers, e.g. point defects, real spin defects and molecular defects, with the latter two characterized by additional internal degrees of freedom. The static and dynamic behaviour of the CN-radical, substituted into Alkali-Halides has been studied very extensively in the last decade with a variety of techniques including thermal conductivity measurements [1], ultrasonic investigations [2], high resolution IR

spectroscopy under applied stress [3, 4], Raman [5] and inelastic neutron scattering [6]. These investigations have been performed on rather dilute concentrations of CN defects, in the order of $10^{19} - 10^{20}$ CN^-/cm^3 , showing that the CN molecule exhibits a variety of excitations like tunneling, hindered rotations and librations. Furthermore it has been demonstrated that the interactions between the internal modes of the CN-dumbbell and the phonons is large and effects on the phonon spectrum are easily detectable. The ultrasonic results of Byer and Sack on $\text{KCl}:\text{CN}$ and $\text{KBr}:\text{CN}$ [2] reveal that sound waves of E_g symmetry i.e. waves which propagate along $[110]$, being polarized in $[1\bar{1}0]$ and which have a sound velocity proportional to $\sqrt{(c_{11} - c_{12})/2}$, interact most strongly with molecular excitations at

* Research supported by the BMFT, W.-Germany

energies of the order of 0.4 THz, while transverse sound waves of T_{2g} symmetry, i.e. waves which propagate along $[100]$ with a velocity proportional to $\sqrt{c_{44}}$, couple to excited states of much lower energy. These observations were supported by Raman measurements on KBr:CN, showing a well resolved band at the same energy of 0.4 THz for the E_g symmetry, while the spectrum in T_{2g} symmetry showed a monotonic tailing off towards zero energy [5], again in agreement with the ultrasonic results. Finally, the direct observation of the mode coupling in E_g symmetry was achieved by neutron scattering experiments with a resonance at 0.45 THz.

While the information on these extremely dilute systems is quite complete the situation for the related mixed crystals $\text{KBr}_{1-x}(\text{CN})_x$ and $\text{KCl}_{1-x}(\text{CN})_x$ is less clear. Raman studies [7] detected at 10 K a shift of the rotational excitation spectrum as a function of the concentration x in both systems. These experiments also indicated the existence of pairs and triplets of coupled CN^- ions. Brillouin scattering data [8] showed that the velocity of the T_{2g} symmetry sound wave passed through a minimum as a function of temperature. This behaviour was explained by Michel et al. [9] in terms of a coupling of the translational lattice modes to orientational relaxations. Very recent inelastic neutron scattering experiments [10] on $\text{KBr}_{0.5}(\text{CN})_{0.5}$ showed a similar temperature dependence of the $[\xi 00]$ TA phonon mode, but from the analysis of the line shapes it was concluded that the theory of Michel et al. could not explain these observations. The authors suggested that their results might be an indication for the formation of a 'glass'-phase at low temperatures as proposed by Fischer and Klein [11].

The situation for the pure molecular crystal KCN is also far from being clear. The greatest obstacle for a deeper understanding of KCN is probably due to the fact that this system exhibits the NaCl-structure only above 168 K. Thus the information on the dynamics of the CN^- -molecule in an environment comparable to that of the dilute system can only be obtained at relative high temperatures where already a large number of molecular states is thermally excited. Inelastic neutron scattering experiments of Rowe et al. [12] on the long wave length T_{2g} symmetry modes were again explained by a coupling of a relaxational type. An extension of the neutron experiment to short wave lengths by Loidl et al. [13] showed, however, that the phonon hybridize with a broad, almost overdamped band of molecular excitations centered at 1.5 THz.

We felt that there exists a gap of information in an intermediate concentration range and tried to collect phonon data in different symmetry directions in or-

der to determine the rotational excitations of the CN^- -molecules via their coupling to the translational modes. In this article we present data of the mixed crystals $\text{KBr}_{1-x}(\text{CN})_x$ with concentrations $x=0.04$ and $x=0.14$ collected by inelastic neutron scattering and by ultrasonic experiments.

2. Inelastic Neutron Scattering Experiments

Good quality single crystals of $\text{KBr}_{1-x}(\text{CN})_x$ of about 1 cm^3 were grown by F. Rosenberger in the Crystal Growth Laboratory of the University of Utah from zone refined KBr and KCN materials. The concentrations of CN^- ions in KBr as determined by chemical analysis were 4% and 14%, the lattice constants at room temperature were 6.59 \AA and 6.572 \AA respectively. The mosaic spread of both crystals was less than 0.2° . The measurements were performed on the triple axis spectrometers IN2 and IN3, situated at the thermal neutron beam tubes at the high flux reactor of the ILL, Grenoble, and on the triple axis spectrometer at the reactor FR2 at the KFA Karlsruhe. All measurements were carried out with incident neutron energies at approximately 13.7 meV using pyrolytic graphite monochromators and filters. At IN3 and at the instrument at Karlsruhe we used vertically bent monochromators, IN2 is equipped with a double monochromator. For most of the measurements the analyser system was chosen to be pyrolytic graphite, for some high resolution scans a Zn(002) analyser was used. The horizontal collimation was varied between $120' - 30' - 30' - 30'$ and $20' - 20' - 20' - 30'$. All data were collected in the (001)-plane of the crystal using the constant-Q mode of operation.

2.1. Phonons in E_g Symmetry

Figures 1 to 4 focus on acoustic modes with E_g character, i.e. phonons propagating along the $[110]$ -direction and being polarized in the $[1\bar{1}0]$ -direction. Figure 1 shows the line shapes of scattered neutron groups for a series of reduced wave vector components in $\text{KBr}_{0.96}(\text{CN})_{0.04}$ at 6 K. One observes a typical coupled mode picture, where the molecular excitations gain intensity from the phonon mode around the resonance at about $\xi=0.125$.

At the CN concentrations investigated in this work we expect to see the molecular excitations in an inelastic neutron scattering experiment only indirectly via their admixture to the translational sta-

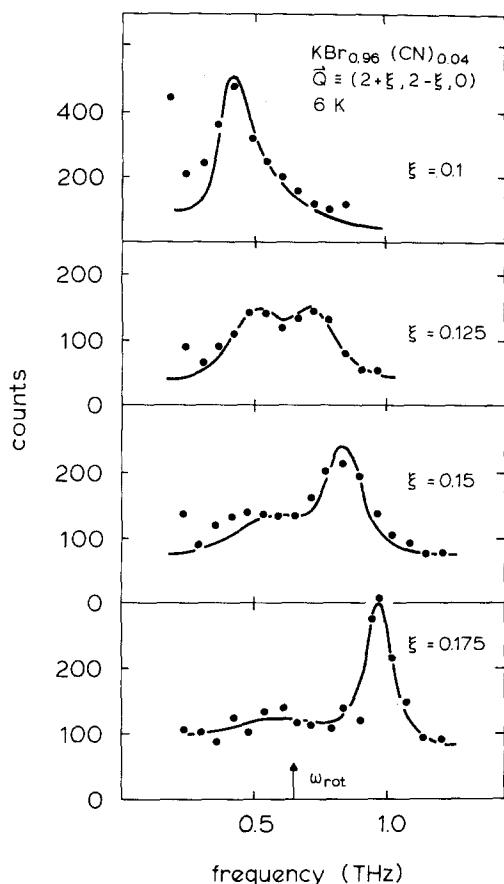


Fig. 1. Constant $-Q$ scans of transverse modes with $q=[110]$ and $e=[1\bar{1}0]$ in $\text{KBr}_{0.96}(\text{CN})_{0.04}$ at 6 K for different phonon vectors. The solid lines represent the fits of the singlet-singlet model involving only one rotational transition. The increase of the intensity towards zero energy transfer is due to Bragg contamination

tes. This is consistent with the experimental findings, that for $\xi \geq 0.3$ there is no extra intensity other than the phonon like excitation. Figure 2 shows the temperature dependence of the coupled modes of the same branch at the resonance ($\xi=0.125$). With increasing temperature the splitting of the double peak structure decreases and at 60 K and above a single peak, considerably broader than the experimental resolution is observed. The enhanced width of the phonon peak could be followed up to room temperature. It will be later shown in the analysis, that the absence of the splitting at higher temperatures can be explained because the driving force of the interaction, the population difference between ground state and first excited state of the molecule decreases with increasing temperature. Figure 3 summarizes the most essential results of $\text{KBr}_{0.96}(\text{CN})_{0.04}$ in E_g symmetry. At room temperature the pure translational character of the excitations dominates with small

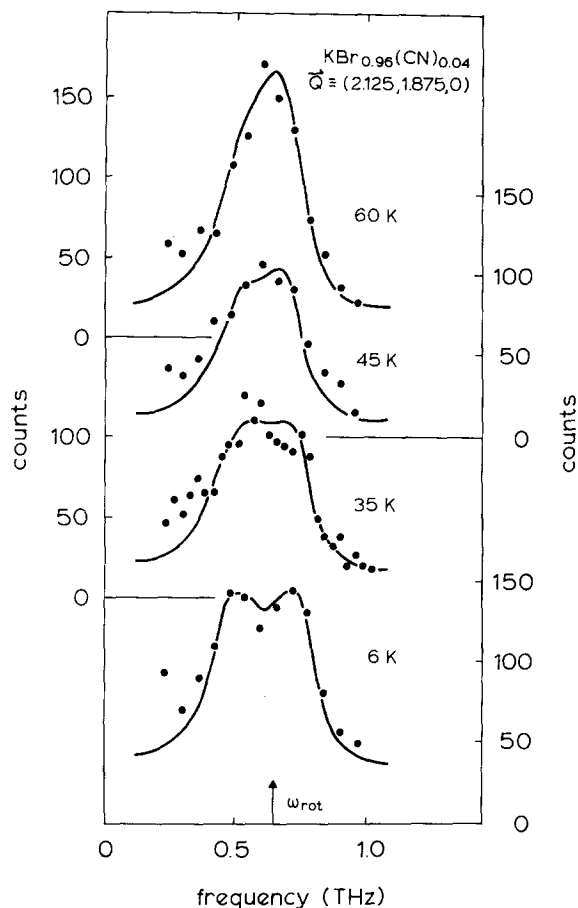


Fig. 2. Temperature dependence of the scattered neutron groups at $Q=(2.125, 1.875, 0)$ in $\text{KBr}_{0.96}(\text{CN})_{0.04}$. The solid lines represent fits of the singlet-singlet model to the experimental data

effects on the line-widths as crossing the resonance region. At 6 K a coupled mode picture with a rotational excitation at $\omega_R=0.65$ THz describes the experimental data in a satisfactory way. In Fig. 4 some results of $\text{KBr}_{0.86}(\text{CN})_{0.14}$ at 10 K along $[\xi\xi 0] T_2 A$ are shown. Clearly one observes a similar behaviour as in the crystal with 4% CN, but now the resonant mixing is shifted to higher energies namely from 0.65 THz to approximately 1.15 THz.

2.2. Phonons in T_{2g} Symmetry

While the inelastic neutron scattering data in E_g symmetry are well described by a coupling of the phonons to a single molecular excitation, the excitation in T_{2g} symmetry propagating along $[100]$ and polarized along $[010]$ exhibit a more complex behaviour. In $\text{KBr}_{0.96}(\text{CN})_{0.04}$ the line shapes of the

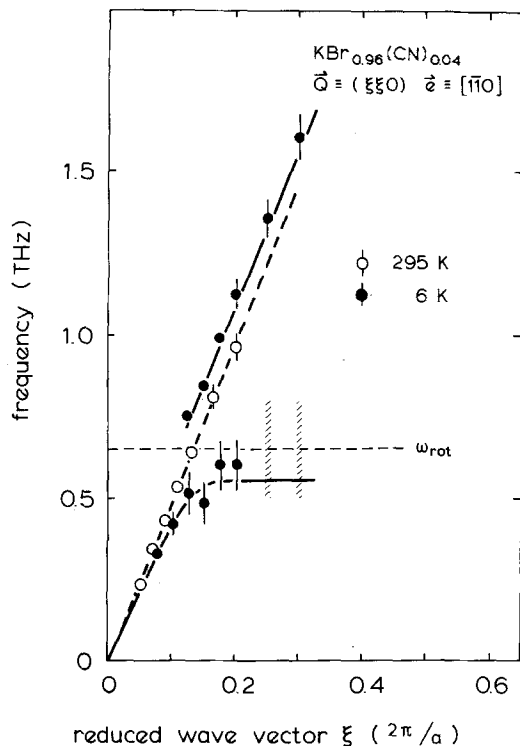


Fig. 3. Phonon dispersion of coupled modes propagating along $[110]$ being polarized in $[\bar{1}\bar{1}0]$ in $\text{KBr}_{0.96}(\text{CN})_{0.04}$ around the resonance frequency ω_R (\bullet 6 K, \circ 295 K). The solid line is the result of our model, the dashed lines are the underlying uncoupled excitations

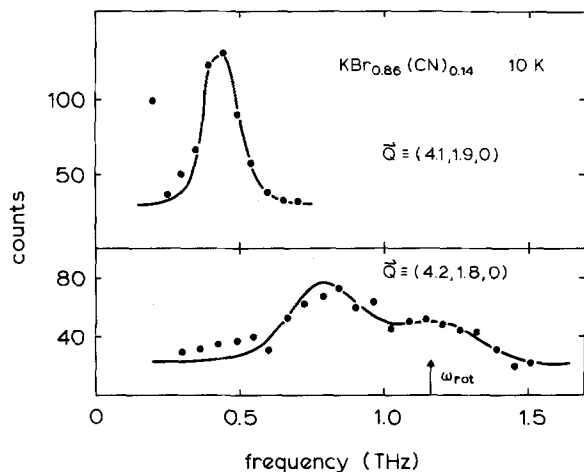


Fig. 4. Constant $-Q$ scans of transverse modes with $\mathbf{q}=[110]$ and $\mathbf{e}=[\bar{1}\bar{1}0]$ in $\text{KBr}_{0.86}(\text{CN})_{0.14}$. The solid lines are the results of fits using a singlet-singlet model

scattered neutron groups show distinct single peak structures at 300 K as well as at 6 K. Table 1 presents a summary of these measurements including the results of Woods et al. [15] in pure KBr at 90 K. Note that the room temperature data of the mixed system

Table 1. The phonon frequencies along $[\xi 00]TA$ in $\text{KBr}_{0.96}(\text{CN})_{0.04}$ at 295 K and at 6 K compared to pure KBr at 90 K [9]

q/q_{ZB}	ω (THz)		
	KBr	$\text{KBr}_{0.96}(\text{CN})_{0.04}$	
	90 K	295 K	6 K
0.1		0.22 ± 0.01	
0.2		0.41 ± 0.01	0.41 ± 0.01
0.25			0.53 ± 0.02
0.3	0.61 ± 0.03	0.60 ± 0.02	0.62 ± 0.02
0.35			0.72 ± 0.02
0.4	0.77 ± 0.02	0.76 ± 0.01	0.80 ± 0.02
0.5	0.90 ± 0.03	0.92 ± 0.01	0.95 ± 0.02
0.8	1.21 ± 0.02	1.21 ± 0.02	
1.0	1.25 ± 0.02	1.26 ± 0.02	

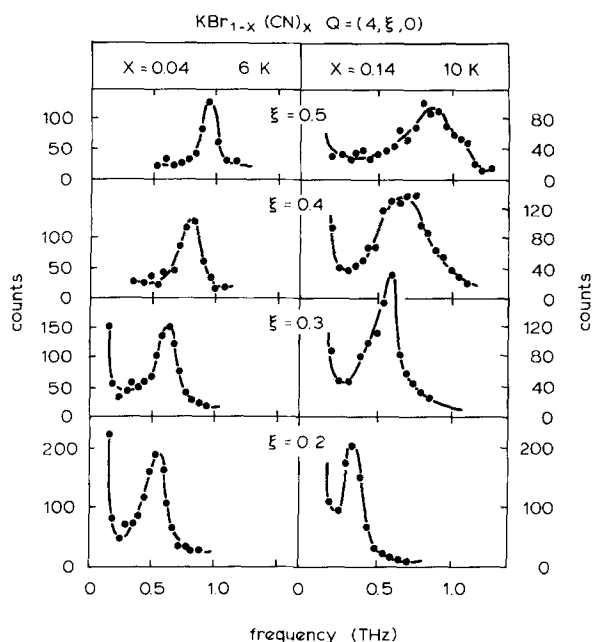


Fig. 5. Constant Q scans of transverse modes along $[100]$ in $\text{KBr}_{0.96}(\text{CN})_{0.04}$ and $\text{KBr}_{0.86}(\text{CN})_{0.14}$ at 6 K and 10 K respectively. The solid lines merely serve as guides to the eye

coincide with the 90 K data of pure KBr, whereas the 6 K data are shifted systematically to higher frequencies, although the magnitude of the shift is almost comparable to the experimental accuracy. If one accepts that these shifts result from a coupling of the phonons to the internal modes one has to conclude that the resonance occurs below 0.4 THz, which is outside the frequency range that could be probed in the present experiment. This conclusion would be in agreement with the ultrasonic [2] and Raman results on the very dilute system mentioned above [5, 7]. Turning over to the crystal with the higher CN^-

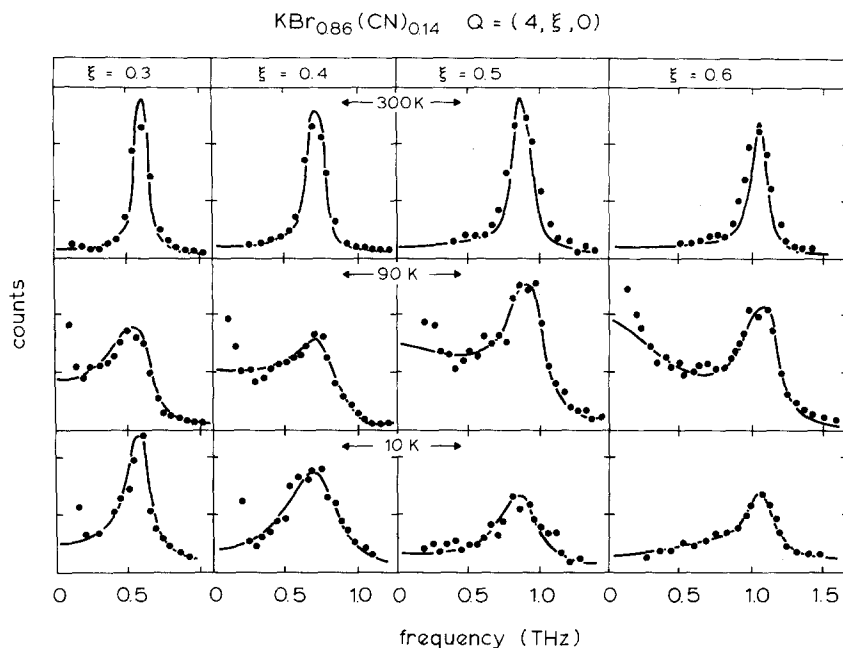


Fig. 6. Constant $-Q$ scans for transverse modes along $[100]$ in $\text{KBr}_{0.86}(\text{CN})_{0.14}$ at 300 K, 90 K and 10 K. The solid lines are the results of fits using a three level scheme of the molecular excitations. The extra intensity at zero energy transfer is only partly due to elastic incoherent scattering. We have been unable to determine correctly the temperature dependence of the quasielastic component, since the scans at different temperatures have been performed at different instruments

Table 2. The phonon frequencies along $[\xi 00] TA$ in $\text{KBr}_{0.86}(\text{CN})_{0.14}$ at 295 K, 90 K and 10 K

q/q_{zB}	ω (THz)		
	295 K	90 K	10 K
0.1	0.225 ± 0.02	0.175 ± 0.03	
0.2	0.415 ± 0.01	0.335 ± 0.03	0.35 ± 0.02
0.3	0.59 ± 0.01	0.52 ± 0.03	0.53 ± 0.02
0.4	0.74 ± 0.02	0.72 ± 0.05	0.70 ± 0.05
0.5	0.91 ± 0.02	0.91 ± 0.03	0.85 ± 0.03
0.6	1.04 ± 0.02	1.07 ± 0.03	1.05 ± 0.03
0.7	1.15 ± 0.02	1.16 ± 0.02	1.15 ± 0.02
0.8	1.24 ± 0.02	1.25 ± 0.02	1.24 ± 0.02
0.9	1.28 ± 0.02	1.31 ± 0.02	1.28 ± 0.02
1.0	1.30 ± 0.02	1.32 ± 0.02	1.33 ± 0.02

concentration, $\text{KBr}_{0.86}(\text{CN})_{0.14}$, the data again in T_{2g} symmetry show a quite complex behaviour. The right hand side of Fig. 5 presents some scans along $[\xi 00]$ at 10 K (which should be compared to those of the crystal with 4% CN at 6 K). Obviously at the higher concentration there appears a considerable phonon line broadening in the frequency range from 0.5 to 1.2 THz. At a first glance the observed data at 10 K could be explained with one broad, strongly damped rotational level at approximately 0.9 THz, since in the presence of strong damping the two peak structure characteristic for coupled modes at the reso-

nance merges in a broad single peak structure. But the temperature dependence of the scattered neutron groups in this branch (Fig. 6) shows that this explanation is incomplete.

If we regard the shape of the phonon signal as a measure for the strength of the coupling of the phonons to the molecular excitations, we note that the interaction at 90 K is even stronger than at 10 K.

This experimental finding cannot be explained by a model which involves only one rotational excitation out of the ground state since in that case the interaction will increase steadily towards lower temperatures. (This situation holds e.g. for the E_g modes in $\text{KBr}_{0.96}(\text{CN})_{0.4}$.) Also the relaxational model cannot account for the observed line shapes correctly. Though it is somewhat crucial how to adjust the relaxation times, one expects sharp and unshifted phonon lines at 10 K (slow relaxation case) [9, 16], both in contradiction to Fig. 6. The failure of the relaxational model was also pointed out by Rowe et al. [10] in $\text{KBr}_{0.5}(\text{CN})_{0.5}$. Two models might give a satisfactory description of the present data: 1) a more complicated level scheme of rotational states, 2) a model with one rotational excitation from the ground state but with a temperature dependent transition matrix element and level spacing. To our knowledge this can only be achieved by a strong coupling between the CN^- ions which eventually leads to an ordering of the CN-dumb-bells. As no

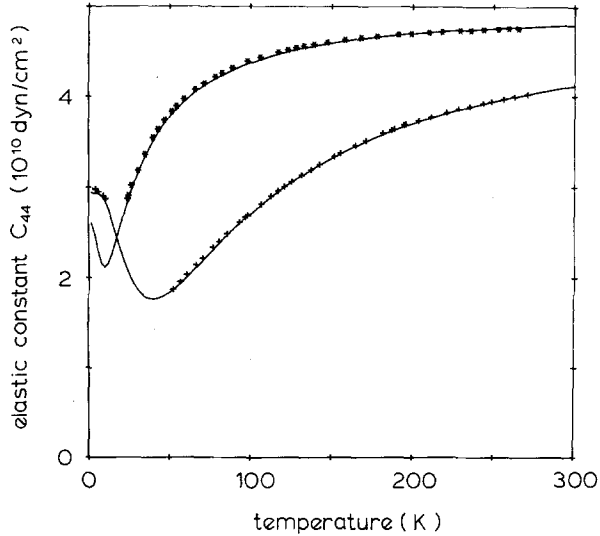


Fig. 7. The temperature dependence of the elastic constant c_{44} in $\text{KBr}_{0.96}(\text{CN})_{0.04}$ (*) and in $\text{KBr}_{0.86}(\text{CN})_{0.14}$ (+). The solid line is the result of the theoretical model involving two rotational excitations, as discussed in the text

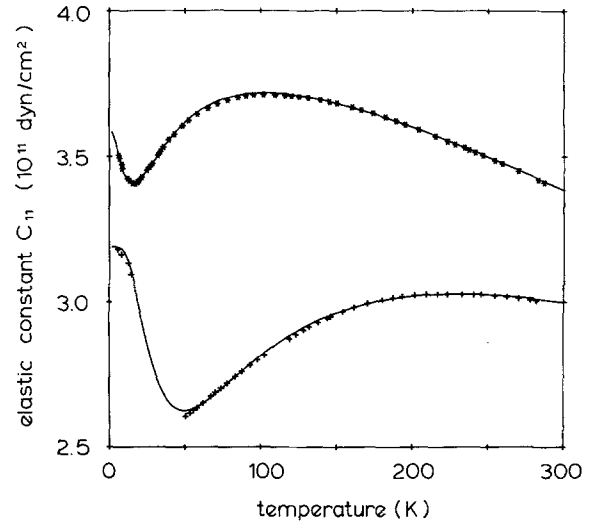


Fig. 8. The temperature dependence of the elastic constant c_{11} in $\text{KBr}_{0.96}(\text{CN})_{0.04}$ (*) and in $\text{KBr}_{0.86}(\text{CN})_{0.14}$ (+). The solid line is the result of the theoretical model

structural phase transition is detectable in the crystal, it has to be a local order in clusters. This would be indicative of a glass phase as pointed out by Rowe et al. [10] and proposed by Fischer and Klein [11]. For the quantitative analysis of the results we follow the first point of view.

In Table 2 we list all the collected phonon frequencies in $\text{KBr}_{0.86}(\text{CN})_{0.14}$ along $[\xi 00]$ TA at 295 K, 90 K and 10 K. Clearly one observes large shifts in the phonon frequencies, which change sign at about half way out to the zone boundary. Again there is a clear indication of mode coupling at frequencies of approximately 0.9 THz.

3. Ultrasonic Measurements

The long wavelength 10 MHz sound waves in both crystals were investigated by ultrasonic measurements using the pulse echo overlap method [17]. The Figs. 7 and 8 show the temperature dependence of the elastic constants c_{11} and c_{44} , corresponding to longitudinal and transverse waves along [100]. These data suggest that the elastic constants pass through a minimum as a function of temperature. This feature is analogous to that obtained by Brillouin scattering experiments on samples with higher CN^- concentrations [8]. The minimum becomes sharper and is shifted to higher temperatures when going from the smaller to the higher concentration. The echoes at temperatures around the minimum were hardly detectable because of an increase of the attenuation. At very low temperatures the sound velocity could be

measured again except for the transverse waves in the 4% sample as shown by the data points.

Again, neither a relaxational model which would yield the undisturbed elastic constant c_0 at the lowest temperatures, nor a simple model with one rotational transition out of the ground state can account for this behaviour. One has to suggest a more complicated level scheme or a 'glass'-picture for a realistic description.

4. Analysis of the Experimental Results

The analysis of the present experimental results follows closely the formalism used recently to explain the neutron line shapes observed in pure KCN [13], based on a theory of Fulde and coworkers [18]. In the limits of small damping the results are similar to that of Wood and Mostoller [19] and of Schober et al. [20]. In the absence of molecular impurities the pure phonon propagator neglecting anharmonic effects is given by

$$D^o(\mathbf{q}, \omega) = \frac{2\omega_0(\mathbf{q})}{\omega_0^2(\mathbf{q}) - \omega^2} \quad (1)$$

where $\omega_0(\mathbf{q})$ is the uncoupled acoustic phonon frequency. The full phonon propagator for the translational modes coupled to rotational excitations is determined by [18]

$$\tilde{D}(\mathbf{q}, \omega) = \frac{2\omega_0(\mathbf{q})}{\omega_0^2(\mathbf{q}) - \omega^2 - 2kA^2\omega_0^2(\mathbf{q}) \cdot g(\omega)} \quad (2)$$

where k is the concentration of CN^- impurities, A^2 is the coupling constant between rotational and translational excitations and $g(\omega)$ is the quadrupolar susceptibility of appropriate symmetry of a single CN^- ion. It can be written as [18]

$$g(\omega) = -\sum_{ij} \frac{\tilde{O}_{ij}^2 A_{ij} (\rho_j - \rho_i)}{\omega^2 - \Delta_{ij}^2 + i\gamma_{ij}\omega} \quad (3)$$

with $\hbar\Delta_{ij}$ the transition energies, γ_{ij} the line broadening for different transitions and \tilde{O}_{ij}^2 describing the strength of the transitions. The ρ_i are thermal occupation numbers of rotator state i divided by the partition function. In analogy to magnetism contributions arising from $i \neq j$ might be called Van Vleck terms, while the diagonal terms $i=j$ yield the Curie terms of the susceptibility.

In contrast to the treatment of KCN the renormalization of the susceptibility due to an effective coupling between the CN^- molecules is neglected because of the low concentrations of the mixed crystals investigated in this study.

The poles of $\tilde{D}(\mathbf{q}\omega)$ describe the excitations in the system. They are given by

$$\omega^2 = \omega_0^2(\mathbf{q}) + 2kA^2 \omega_0^2(\mathbf{q}) \sum_{ij} \frac{\tilde{O}_{ij}^2 A_{ij} (\rho_j - \rho_i)}{\omega^2 - \Delta_{ij}^2 + i\gamma_{ij}\omega}. \quad (4)$$

From this equation one finds the temperature dependence of the sound velocity by dividing (4) by q^2 and taking the limit $\omega \rightarrow 0$

$$v^2 = v_0^2 \left[1 - 2kA^2 \sum_{ij} \frac{\tilde{O}_{ij}^2 (\rho_j - \rho_i)}{\Delta_{ij}} \right] \quad (5)$$

with the sound velocities $v = \omega/|\mathbf{q}|$ and $v_0 = \omega_0(\mathbf{q})/|\mathbf{q}|$. Finally the dynamic structure factor is determined by

$$S(\mathbf{q}, \omega) = \left[1 - \exp\left(-\frac{\hbar\omega}{k_B T}\right) \right]^{-1} \text{Im} \tilde{D}(\mathbf{q}\omega). \quad (6)$$

The temperature dependence of the elastic constants as measured by ultrasonic techniques is described by (5) with $v_0^2 = c_0/\rho$, c_0 being the background elastic constant and ρ the mass density. Finally the temperature dependence of the elastic constants c due to anharmonic phonon interactions is added

$$c = c_0 \left[1 - \alpha \frac{\theta}{e^{\theta/T} - 1} - 2kA^2 \sum_{ij} \tilde{O}_{ij}^2 \frac{(\rho_j - \rho_i)}{\Delta_{ij}} \right] \quad (7)$$

where α is the linear expansion coefficient and θ the Debye temperature. For the latter the value of pure KBr ($\theta = 177$ K) was taken.

For the analysis of the neutron data measured in E_g symmetry we used a very simple form for the molecular susceptibility $g(\omega)$, namely a ground state fol-

lowed by one excited state with a level separation Δ and a line broadening γ . The solid lines in Figs. 1, 2 and 4 show the results of fit to the experimental data using (6) with this assumption. The phonon wave vector dependence in both mixed crystals as well as the temperature dependence of the coupled modes with E_g symmetry in $\text{KBr}_{0.96}(\text{CN})_{0.04}$ are well described. Table 3 summarizes the parameters involved in the fit at the lowest temperatures, namely the background elastic constant c_0 , the level spacing Δ , the line broadening γ and the coupling strength $A^2\tilde{O}^2$. Remarkable is the increase in the level separation by a factor of two by moving from 4% to 14% CN concentration in KBr. This feature is in qualitative agreement with Raman results [7]. One also notes a decrease in the coupling strength. In the temperature range investigated the line broadening shows only an insignificant temperature dependence and increases from 0.4 THz at 6 K to 0.45 THz at 60 K in $\text{KBr}_{0.96}(\text{CN})_{0.04}$, while one notes an increase of the line-widths with increasing CN^- concentration. Equation (4) yields the poles of the coupled modes. The results for $\text{KBr}_{0.96}(\text{CN})_{0.04}$ are drawn as full lines in Fig. 3. The dashed lines represent the uncoupled excitations, where we determined the values of ω_0 with a simple sinusoidal dependence with the initial slope determined by c_0 .

The model which yields a quantitative description of the inelastic neutron scattering data in T_{2g} symmetry in $\text{KBr}_{0.86}(\text{CN})_{0.14}$ and of all our ultrasonic results in $A_{1g} \oplus E_g$ and T_{2g} symmetry consists of three rotational levels at energies $E_0=0$ (ground state), $E_1 = \Delta_1$ (first excited state) and $E_2 = (\Delta_1 + \Delta_2)$ (second excited state). We assume quadrupolar T_{2g} transitions to connect $E_0 - E_1$ with a strength \tilde{O}_1^2 and $E_1 - E_2$ with a strength \tilde{O}_2^2 . Using this level scheme and an averaged line broadening γ for either transition, $S(\mathbf{q}\omega)$ was calculated from (6). The result of these fits are shown as solid lines in Fig. 6 for the neutron data. The parameters as determined by the fitting are listed in the first column of Table 4. It is interesting to note that the level spacings of both transitions are of the same order and somewhat smaller than the level separation in pure KCN [12], while the factors $A^2\tilde{O}^2$ differ by a factor of 10 with the weaker transition

Table 3. The parameters of the singlet-singlet model fitted to the observed neutron line shapes in E_g symmetry in $\text{KBr}_{1-x}(\text{CN})_x$ at 6 K ($x=0.04$) and at 10 K ($x=0.14$)

x		0.04	0.14
c_0	(10^{10} dyn/cm ²)	16	16
Δ	(THz)	0.65	1.15
γ	(THz)	0.4	0.6
$A^2\tilde{O}^2$	(THz)	4.0	2.1

Table 4. The parameters as determined by fitting a model with two rotational transitions to the ultrasonic and inelastic neutron data in T_{2g} symmetry on $\text{KBr}_{1-x}(\text{CN})_x$. The background elastic constants c_0 listed for the two symmetries correspond to c_{11} ($A_{1g} \oplus E_g$) and c_{44} (T_{2g})

Symmetry	Neutron data		Ultrasonic data			
	T_{2g}	T_{2g}	T_{2g}		$A_{1g} \oplus E_g$	
	$x=0.14$	0.04	0.14	0.04	0.14	
c_0 (10^{10} dyn/cm ²)	5.2	5.1	5.15	40.7	38.9	
A_1 (THz)	1.0	0.27	0.9	0.23	1.07	
A_2 (THz)	0.9	0.5	1.65	1.05	1.8	
$A^2 \bar{O}_1^2$ (THz)	1.2	1.65	1.39	0.36	0.69	
$A^2 \bar{O}_2^2$ (THz)	11.5	10.1	12.7	5.2	7.4	
γ (THz)	1.5	—	—	—	—	
α ($10^{-4}/\text{K}$)	—	0.5	0.25	6.6	5.4	

involving the ground state. In pure KCN $A^2 \bar{O}^2$ was determined to be 2.1 THz. The averaged line broadening $\bar{\gamma}$ is 1.5 THz independent of temperature and is just in the same order as in KCN [13].

The overall features of the spectra are easily understood assuming the mode strengths including coupling and transition strengths and the population difference in the rotational states. With decreasing temperature the population differences between excited states runs through a maximum and becomes zero at 0 K. Thus the effect of the upper transition dies out when approaching $T=0$. The line shapes at the lowest temperatures are then only determined by the transition from the ground state. Figure 9 presents the observed frequency shifts (300 K – 90 K data and 300 K – 10 K data) versus the phonon wave vector which is compared to the calculated values using the parameters as determined by the fits to the line shapes. The overall features, in particular the fact that the interaction at 10 K is weaker than at 90 K, are well described.

In $\text{KBr}_{0.96}(\text{CN})_{0.04}$ the interaction of phonons with molecular excitations in T_{2g} symmetry is at frequencies lower than 0.4 THz which could not be reached in the present experiment. The positive frequency

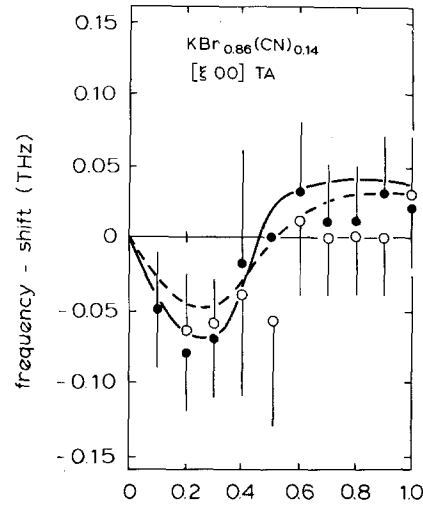


Fig. 9. Observed and calculated frequency shifts in $\text{KBr}_{0.86}(\text{CN})_{0.14}$ for transverse phonons along [100]: \bullet (300 K – 90 K), \circ (300 K – 10 K). The lines are the results of calculations using the three level scheme: solid line (300 K – 90 K), dashed line (300 K – 10 K)

shifts of the scattered neutron groups at 6 K with respect to 300 K for wave vectors $\xi \geq 0.2$ are an indication of this interaction.

With the same model, using (7), the temperature dependence of the elastic constants c_{11} and c_{44} as determined by ultrasonic techniques were fitted. The results are shown as solid lines in the Figs. 7 and 8. The parameters obtained from these fits are also listed in Table 4. The agreement with the values from the neutron scattering results in $\text{KBr}_{0.86}(\text{CN})_{0.14}$ in T_{2g} symmetry is only fair, with the largest discrepancies occurring for A_2 . One has to keep in mind that the ultrasonic measurements are not very sensitive to the level separations A_1 and A_2 . Furthermore, the correlation between the transition probabilities and the excitation energies is high. Taking the parameters which were obtained from the neutron data one achieves a temperature dependence of c_{44} which is very similar to that shown in Fig. 8.

Similar to the neutron scattering results the ultrasonic results indicate an increase of the level spacings

Table 5. The room temperature elastic constants of $\text{KBr}_{1-x}(\text{CN})_x$, KBr (from Ref. 21), KCN (from Ref. 22) in units of 10^{10} dyn/cm². (us = from ultrasonic, n = from neutron experiments)

	KBr	$\text{KBr}_{0.96}(\text{CN})_{0.04}$		$\text{KBr}_{0.86}(\text{CN})_{0.14}$		KCN
	(us)	(us)	(n)	(us)	(n)	(us)
c_{11}	34.8	33.8 ± 0.8	36.5 ± 1.5	30.0 ± 0.8	33.6 ± 1.5	19.2
c_{44}	5.1	4.8 ± 0.2	5.3 ± 0.5	4.1 ± 0.2	4.8 ± 0.5	1.41
$(c_{11} - c_{12})/2$	14.5		13.5 ± 1.5		12.9 ± 1	3.6
c_{12}	5.7		9.3 ± 3		7.8 ± 2.5	12.0

with increasing CN concentration. Finally Table 5 gives a listing of the elastic constants at room temperature of the two mixed crystals as determined from the ultrasonic measurements and from the initial slopes at small phonon wave vectors by inelastic neutron scattering, compared to the elastic constants in pure KBr [21] and in pure KCN [22] as measured with ultrasonic techniques.

In comparing these elastic constants one has to keep in mind that the frequencies in an inelastic neutron scattering experiment probe zero sound, while the ultrasonic experiments measure first sound.

5. Discussion

The present investigation definitely shows that molecular excitations with finite energies exist in $\text{KBr}_{1-x}(\text{CN})_x$ and couple to the phonons. The temperature dependence of the scattered neutron intensities and of the elastic constants of $\text{KBr}_{1-x}(\text{CN})_x$ were quantitatively explained by a coupling of the phonons to the rotational excitations of the CN-molecules. Rather simple forms of the molecular susceptibilities $g(\omega)$ were assumed for the quantitative description. For the E_g symmetry one Van Vleck term was sufficient to explain the experimental results. However, in the $A_{1g} \oplus E_g$ and the T_{2g} symmetries two Van Vleck terms have to be introduced, with the strongest transition connecting the excited states, in order to account for the temperature dependence of the elastic constants and the observed neutron lineshapes.

These assumptions are only justified by the limited amount of information on the molecular system which can be extracted from the neutron and the ultrasonic results. Unfortunately, the spectrum of the molecular excitations in $\text{KBr}_{1-x}(\text{CN})_x$ mixed crystals is yet unknown. It is certainly more complex than assumed here.

Furthermore the present analysis assumes that the molecular system is characterized by the susceptibility of independent CN^- ions, with temperature independent level separations Δ and matrix elements \tilde{O}^2 . For concentrations of several percent one expects, however, from the Raman results an already strong effective coupling between neighbouring CN^- -ions which leads to sets of bound CN^- -pairs, triplets etc., say local CN^- -clusters, which have their own characteristic spectrum of molecular states. The different level spacings which were observed for the 4% and the 14% samples, for the E_g as well as for the T_{2g} symmetry, might be in fact indications that the molecular system is dominated by the contributions of clusters rather than by contributions of isolated CN^- -ions [7]. The crucial question is if the assump-

tion of temperature independent level separations and transition matrix elements is warranted. Changes with temperature could occur if the coupling between the molecules would lead to an orientational ordering of the CN^- -dumb-bells. As no structural phase transitions are detected one could only think of short range order in clusters similar to spin glasses. In that case our analysis should be applicable well below and well above the freezing temperature T_F . The molecular excitation spectrum would change considerably around T_F and the model used would be not applicable if T_F would fall in the temperature range probed in the present experiment. In fact, the minima observed in the elastic constants in the present work and in the Raman studies of rev [8] remind of the cusp of the magnetic susceptibility at the freezing temperature in spin glasses like Cu:Mn. In addition, the growth of the $\omega=0$ intensity in recent neutron scattering experiments on $\text{KBr}_{0.5}(\text{CN})_{0.5}$ [10] might indicate the onset of short range ordering, a fact which is again analogous to the results in spin glasses.

The problem which is encountered in attempts to describe this situation quantitatively is that for the intermediate concentrations of interest neither the dilute limit nor the concentrated limit is applicable. A qualitative insight into the possible dynamics of the molecules can, however, be obtained by investigating the limit of high concentrations where the effective coupling between the CN-molecules can be described by its Fourier transform $J(\mathbf{q})$. Assuming that the susceptibility of a single molecule is given by a single Van Vleck-term (characterized by the level spacing Δ and the matrix elements \tilde{O}^2) the molecular excitation will show a temperature dependence which is e.g. familiar from singlet-ground-state magnetism. The excitation will start at an energy Δ at high temperatures and soften, at the ordering wave vector, towards the ordering temperature T_c . Below T_c it recovers to energies higher than Δ in the finite molecular field while at the same time the mode strength of this excitation decreases in favour of an ordered moment (at $\omega=0$). A coupling of this soft mode to the phonon system could qualitatively explain the results of $\text{KBr}_{1-x}(\text{CN})_x$ i.e. the minima of the elastic constants and the onset of static intensity of the neutron scattering experiments of Rowe et al. at about T_F and the change of strong coupling at 90 K to a weaker coupling at 10 K in the T_{2g} neutron results, but it also leaves a question open, why we did not detect any marked changes in the line shapes of phonons in E_g symmetry in passing through the 'freezing temperature' as determined by the minimum in the temperature dependence of the elastic constant c_{11} in $\text{KBr}_{0.96}(\text{CN})_{0.04}$.

6. Conclusions

In this paper detailed inelastic neutron scattering and ultrasonic results on the coupled rotational and translational modes in the mixed crystals $\text{KBr}_{1-x}(\text{CN})_x$ have been reported. The E_g and T_{2g} symmetry modes showed quite different behaviour. In the E_g symmetry, only one molecular excitation involving the ground state yields a satisfactory description of the observed data. As the line broadening of the rotational transition is comparatively small, a coupled mode picture with two peak structure near the resonance is observed. These findings are similar to the behaviour observed in the very dilute compound $\text{KCl}:\text{CN}$ in the same symmetry [6]. The level separation increases from 0.65 THz to 1.15 THz when moving from 4% CN to 14% CN in KBr . Presumably this change is due to the existence of bound pairs of CN-molecules at the higher concentration. The coupled modes in T_{2g} symmetry exhibit a more complex behaviour showing at 90 K a stronger interaction than at 300 K or at 10 K. A level scheme with three molecular excitations with the strongest transition from the first to the second excited state yields a good description of the experimental data. Again one notes an increase in the level separation with increasing concentration. The line broadening of the rotational transitions in this symmetry is large and exceeds the level spacings. The value of 1.5 THz for an averaged line broadening is just the value recently determined for pure KCN [13]. As the rotational modes are heavily damped no clear multiplex structure can be seen in the neutron line shapes.

A competing picture, with a concentration dependent freezing temperature and a low temperature glass phase, earlier proposed by Rowe et al. [10], was discussed qualitatively.

References

- Hetzler, Jr. M.C., Walton, D.: Phys. Rev. B **8**, 4801 (1973)
- Byer, N.E., Sack, H.S.: phys. stat. sol. (b) **30**, 569 (1968)
- Lüty, F.: Phys. Rev. B **10**, 3677 (1974)
- Beyeler, H.U.: Phys. Rev. B **11**, 3078 (1978)
- Durand, D., Lüty, F.: phys. stat. sol. (b) **81**, 443 (1977)
- Walton, D., Mook, H.A., Nicklow, R.M.: Phys. Rev. Lett. **33**, 412 (1974)
- Durand, D., Lüty, F.: Ferroelectrics **16**, 205 (1977)
Durand, D.: unpublished
- Satija, S.K., Wang, C.H.: Solid State Commun. **28**, 617 (1978)
- Michel, K.H., Naudts, J., De Raedt, B.: Phys. Rev. B **18**, 648 (1978)
- Rowe, J.M., Rush, J.J., Hinks, D.G., Susman, S.: Phys. Rev. Lett. **43**, 1158 (1979)
preliminary results in $\text{KBr}_{0.75}(\text{CN})_{0.25}$ have been communicated by the same group
Rowe, J.M., Rush, J.J., Chesser, N.J., Hinks, D.L., Susman, S.: J. Chem. Phys. **68**, 4320 (1978)
- Fischer, B., Klein, M.W.: Phys. Rev. Lett. **40**, 455 (1978)
- Rowe, J.M., Rush, J.J., Chesser, N.J., Michel, K.H., Naudts, J.: Phys. Rev. Lett. **40**, 455 (1978)
- Loidl, A., Knorr, K., Daubert, J., Dultz, W., Fitzgerald, W.J.: Z. Physik (to be published)
- Beyeler, H.U.: phys. stat. sol. (b) **52**, 419 (1972)
- Woods, A.D.B., Brockhouse, B.N., Cowley, R.A., Cochran, W.: Phys. Rev. **131**, 1025 (1963)
- Yamada, Y., Taktera, H., Huber, D.L.: J. Phys. Soc. Jap. **36**, 641 (1974)
- Papadakis, E.P.: J. Appl. Phys. **35**, 1474 (1964)
- Fulde, P.: Handbook of the Physics and Chemistry of Rare Earths. Gschneider, K.A., Eyring, L. (eds.), p. 295, Amsterdam: North Holland Publ. 1978
Dohm, V., Fulde, P.: Z. Physik B **21**, 369 (1975)
- Wood, R.F., Mostoller, M.: Phys. Rev. Lett. **35**, 45 (1975)
- Schober, H.R., Tewary, V.K., Dederichs, P.H.: Z. Physik B **21**, 255 (1975)
- Hausühl, S.: Z. Physik **159**, 223 (1960)
- Hausühl, S.: Solid State Commun. **13**, 147 (1973)

A. Loidl
R. Feile
K. Knorr
Institut für Physik
Johannes Gutenberg Universität Mainz
Jakob-Welder-Weg 11
D-6500 Mainz
Federal Republic of Germany

B. Renker
Institut für Angewandte Kernphysik
Kernforschungszentrum Karlsruhe GmbH
Postfach 3640
D-7500 Karlsruhe
Federal Republic of Germany

J. Daubert
Physik-Department
Technische Universität München
D-8046 Garching bei München
Federal Republic of Germany

D. Durand
Faculté des Sciences
Université de Metz
F-57000 Metz
France

J.B. Suck
Institut Max von Laue-Paul Langevin
156 X
F-38042 Grenoble Cedex
France